

Investigating the scaling of higher-order flows in relativistic heavy-ion collisions

Chun-Jian Zhang^{1,2} and Jun Xu^{1,*}¹*Shanghai Institute of Applied Physics, Chinese Academy of Sciences, Shanghai 201800, China*²*University of Chinese Academy of Sciences, Beijing 100049, China*

(Received 11 November 2015; published 8 February 2016)

The modified number of constituent quark (NCQ) scaling $v_n/n_q^{n/2} \sim K E_T/n_q$ for mesons and baryons and the scaling relation $v_n \sim v_2^{n/2}$ for higher-order anisotropic flows, which were observed experimentally, have been investigated at the top energy of Relativistic Heavy-Ion Collider. It has been found that the modified NCQ scaling cannot be obtained from the naive coalescence even by taking into account event-by-event fluctuations but may be due to hadronic afterburner or thermal freeze-out. In addition, we observed that the behavior of the $v_n/v_2^{n/2}$ ratio is sensitive to the partonic interaction. Further insights about the relation between the two scalings are discussed.

DOI: [10.1103/PhysRevC.93.024906](https://doi.org/10.1103/PhysRevC.93.024906)

I. INTRODUCTION

Relativistic heavy-ion collisions provide a useful way of studying the phase which may exist at extremely high energy densities on earth. Collectivity is one of the main pieces of evidence of the produced dense matter, named quark-gluon plasma (QGP), produced in the Relativistic Heavy-Ion Collider (RHIC) [1–4]. Due to the almond shape of the produced QGP in noncentral collisions, there are more freeze-out particles moving in plane than out of plane, leading to the so-called elliptic flow (v_2). Generally, the anisotropic flow is believed to be mostly produced at the early stages of the collision when the interaction is strongest. The number of constituent quark (NCQ) scaling law $v_2/n_q \sim p_T/n_q$ or $v_2/n_q \sim K E_T/n_q$ [5–10], where p_T and $K E_T$ are respectively the transverse momentum and transverse kinetic energy, shows that the underlining mechanism for hadron elliptic flow is from partons, as baryons and mesons are scaled by their number of constituent quark numbers n_q . The NCQ scaling can be well explained by the coalescence model [11–15], typically by assuming that hadrons are formed from the combination of constituent quarks whose distance in momentum space is small [16,17]. The coalescence or recombination mechanism also automatically results in the relation $v_4 \sim v_2^2$ from the leading order [17], which originates actually from the partonic level [18]. Although the above coalescence picture works well at intermediate p_T or $K E_T$, it has been observed that the collective flows of light and heavy hadrons obey the mass ordering at low p_T , showing the thermalization of different species of particles in the medium [6,8,9], and this can usually be explained by a blast wave model [19] or the Cooper-Frye freeze-out condition [20] in the hydrodynamic model.

Recently, it was realized that the initial spatial distribution of QGP is not a smooth one but has density fluctuations [21,22]. The initial anisotropy in coordinate space can develop into the final anisotropy in momentum space as a result of QGP interaction. This leads to the redefinition of higher-order harmonic flows with respect to their event plane or participant

plane, especially the odd-order harmonic flows [21–27]. It was further found that the scaling of the higher-order harmonic flows is modified to $v_n/n_q^{n/2} \sim K E_T/n_q$, mostly from least square fit [28]. The above modified NCQ scaling for higher-order flows might stem from the relation between flows of different orders $v_n \sim v_2^{n/2}$ [29], although the relationship between the two scalings has never been clarified. It was further found that the coefficient is nearly a constant with respect to transverse momentum but increases with decreasing collision centrality [29,30]. Studying the scaling relation between flows of different orders is helpful in understanding the behavior of the initial eccentricities [31,32], the viscous property of QGP [33], and the acoustic nature of anisotropic flows [30], while it is known that the hadronization may affect the scaling coefficient. Since in the previous recombination model [17] the initial density fluctuation was not considered, it is of great interest to include event plane corrections in the quark coalescence model. In the present work we carry out such a study to see whether the corrections can lead to the modified scaling of the higher-order harmonic flows $v_n/n_q^{n/2} \sim K E_T/n_q$. We also try to investigate the scaling $v_n \sim v_2^{n/2}$ and understand the relation between the two scalings. We will see that the modified scaling relation can originate from the hadronic afterburner or thermalization in the freeze-out stage instead of higher-order corrections in the coalescence picture.

This paper is organized as follows. In Sec. II we briefly describe the models and formalism used in the present study, i.e., a multiphase transport (AMPT) model, the quark coalescence formalism with event-by-event fluctuations, and the thermal blast wave model. In Sec. III we investigate the scaling law of $v_n/n_q^{n/2} \sim K E_T/n_q$ and $v_n \sim v_2^{n/2}$ in detail by using the theoretical tools presented in Sec. II. Finally, a conclusion is given in Sec. IV.

II. MODELS AND FORMALISM

In the present study, the AMPT model is used to give a reasonable final parton phase-space distribution and serves as a useful tool to test the effect of hadronic afterburner. With the collective flows of partons in the freeze-out stage, a naive

*Corresponding author: xujun@sinap.ac.cn

quark coalescence model is used to generate the hadronic flows analytically in the spirit of Ref. [17] by taking into account event-by-event fluctuations. To study the scaling law from thermal freeze-out other than the coalescence picture, a generalized blast wave model with higher-order flows is also described for the convenience of discussion.

A. AMPT model

The AMPT model [34] has been widely used in theoretical studies or experimental simulations. For Au+Au collisions at $\sqrt{s_{NN}} = 200$ GeV, which is the system in the present study, the string melting version of AMPT is used. The initial parton information is generated from the heavy-ion jet interaction generator (HIJING) model [35] by melting hadrons into their valence quarks and antiquarks. The evolution of the partonic phase is then modeled by Zhang's parton cascade (ZPC) [36], where the interaction between quarks or antiquarks is effectively described by two-body scatterings. The freeze-out time of a parton is given by its last scattering, after which the distance between two quarks is out of their scattering cross section. The phase-space information at this stage is used for hadronization in AMPT and the analytical coalescence as given in the next subsection. In the current version of AMPT, the hadronization is described by a coalescence model in which quarks or antiquarks that are close in coordinate space can form hadrons, and the hadron species depends on the flavors of its valence quarks and their invariant mass. In this way the space anisotropy from the final partonic stage to the initial hadronic stage is preserved, while the distance between valence quarks in momentum space may not be small. We will return to this point later. After hadronization, the hadronic evolution is described by a relativistic transport (ART) model [37], where elastic and inelastic scatterings as well as resonance decays of hadrons are properly treated. We will use ART as a tool to investigate the hadronic afterburner effect on the scaling law of collective flows in the present work.

B. Analytical coalescence

The above described AMPT model is a dynamical transport model. To have some insights into the quark coalescence mechanism from a more easily handled way, here we give the analytical coalescence formalism by extending the previous work in Ref. [17] and taking into account event-by-event fluctuations. We start from the following azimuthal distribution of partons at freeze-out stage:

$$f(p_T, \phi) \propto 1 + 2 \sum_{n=1}^{\infty} v_n(p_T) \cos[n(\phi - \psi_n)], \quad (1)$$

where ϕ is the azimuthal angle, v_n is the n th-order anisotropic flow, and ψ_n is the corresponding event plane. In the present study, the partonic flow v_n can be obtained from the AMPT model with ψ_n determined by the parton phase-space distribution at the freeze-out stage.

In the naive analytical coalescence picture, the momentum distribution of quarks inside hadrons is neglected, and the hadron yield is proportional to the quark density to the power of its constituent quark number. This can be viewed as a

limit in the dynamical coalescence method [11,12] where the momentum part of the Wigner function is a δ function instead of a Gaussian form. In this limit the azimuthal distribution of mesons and baryons can be expressed respectively as

$$F(2p_T, \phi) \propto f^2(p_T, \phi) \propto 1 + 2 \sum_{n=1}^{\infty} V_n(2p_T) \cos[n(\phi - \psi_n)],$$

$$\tilde{F}(3p_T, \phi) \propto f^3(p_T, \phi) \propto 1 + 2 \sum_{n=1}^{\infty} \tilde{V}_n(3p_T) \cos[n(\phi - \psi_n)],$$

where the anisotropic flows of mesons and baryons can be calculated respectively from

$$V_n(2p_T) = \frac{\int_0^{2\pi} \cos(n\phi - n\psi_n) F(2p_T, \phi) d\phi}{\int_0^{2\pi} F(2p_T, \phi) d\phi} \quad (2)$$

and

$$\tilde{V}_n(3p_T) = \frac{\int_0^{2\pi} \cos(n\phi - n\psi_n) \tilde{F}(3p_T, \phi) d\phi}{\int_0^{2\pi} \tilde{F}(3p_T, \phi) d\phi}. \quad (3)$$

We expand the value of n up to 4 in this work. The detailed expressions of meson and baryon flows as well as their various ratios in terms of the partonic flows and event planes are given in Appendix A.

The original method proposed by Kolb *et al.* [17] can be considered as a limit from a smooth initial condition with $\psi_n = 0$, while in the present study the phase space distribution of freeze-out partons is generated by AMPT model calculation and thus the event-by-event fluctuation is included. Comparing the flow expressions of mesons and baryons [Eqs. (A6)–(A8) and (A13)–(A15)] with those in Ref. [17], one finds that the main difference is the event plane angle correlation. Since the cosine of the event plane angle correlation is always smaller than 1, one expects that only the leading terms are important, as in Ref. [17].

Despite of the success of the dynamical coalescence model in explaining the scaling law of hadron flows [11–15] in relativistic heavy-ion collisions as well as light cluster production [38] in intermediate-energy heavy-ion collisions, this model suffers from an energy conservation problem at lower transverse momenta but works reasonably well at intermediate transverse momenta. On the other hand, the naive coalescence method provides us with an opportunity to study the hadronization in a semianalytical way. The intuitive picture of the naive coalescence method can serve as a baseline for the comparison with results from other models to be discussed in the following.

C. Blast wave model

In the present subsection, we briefly review the blast wave model, which can be viewed as a simplified version of the Cooper-Frye freeze-out condition used in the hydrodynamic model. In this sense, the initial hadrons right after hadronization are assumed to be in thermal and chemical equilibrium, and the medium is undergoing a collective expansion. In the standard version of the blast wave model [19], particles are emitted perpendicularly from the surface of an elliptical

medium in the transverse plane representing the azimuthal distribution in the midrapidity region, and this model can be used to fit the p_T spectra and the v_2 of different particle species reasonably well, by neglecting the hadronic afterburner effect. The standard version of the blast wave model can be easily generalized to include the higher-order collective flows and anisotropies of the system right after hadronization [28].

In the generalized blast wave model, the Lorentz-invariant thermal distribution can be expressed as

$$f(\vec{r}, \vec{p}) \propto \exp(-p^\mu u_\mu / T_f), \quad (4)$$

where T_f is the freeze-out temperature, $p^\mu = \{E, p_x, p_y, p_z\}$ is the four-momentum, $u_\mu = \gamma\{1, \rho_x, \rho_y, \rho_z\}$ is the four-velocity field with $\gamma = 1/\sqrt{1 - \rho_x^2 - \rho_y^2 - \rho_z^2}$, and the n th-order azimuthal velocity as well as the spatial density anisotropies are respectively expressed as

$$\rho(\phi, r) = \rho_0 \left\{ 1 + \sum_{n=1}^{\infty} \rho_n \cos[n(\phi - \psi_n)] \right\} \frac{r}{R}, \quad (5)$$

$$S(\phi) = 1 + \sum_{n=1}^{\infty} s_n \cos[n(\phi - \psi_n)]. \quad (6)$$

In the above, ρ_0 is the radial flow, R is the size of the emission source, and ψ_n is the event plane but is set to 0 in the blast wave study. In the hydrodynamical calculation, both the velocity and spatial anisotropy coefficients ρ_n and s_n can be consistently obtained. Since in the present study we will only consider the modified NCQ scaling $v_n/n_q^{n/2} \sim KE_T/n_q$ for mesons and baryons using the generalized blast wave model, we simply set $\rho_n = 0.43$ and $s_n = -0.05$ fm to be the same for different orders n . The values of the other parameters are taken from Ref. [39] used to describe the initial hadron distribution before hadronic evolution in Au+Au collisions at $\sqrt{s_{NN}} = 200$ GeV, and they are $T_f = 175$ MeV, $R = 5.0$ fm, and $\rho_0 = 0.55$.

III. RESULTS AND DISCUSSIONS

We now investigate the scaling of higher-order anisotropic flows v_n in detail. The standard event-plane method in calculating v_n is detailed in Appendix B, where the autocorrelation between the particle and the event plane is removed, and it is found that the resolution correction is very small. In our previous work [26], a partonic scattering cross section of 1.5 mb in the AMPT model is used to describe the experimental anisotropic flows from two-particle cumulant method in Au+Au collisions at $\sqrt{s_{NN}} = 200$ GeV. Since the purpose of this study is not to fit the experimental data but to understand the origin of the scaling law of higher-order harmonic flows, we will compare the results from partonic scattering cross sections of 1.5 and 10 mb, and will mainly focus on the results from the cross section of 10 mb with a larger collectivity effect.

A. The modified NCQ scaling $v_n/n_q^{n/2} \sim KE_T/n_q$

First of all, we investigate numerically whether the higher-order corrections from event-by-event fluctuations in the analytical coalescence scenario can be responsible for the

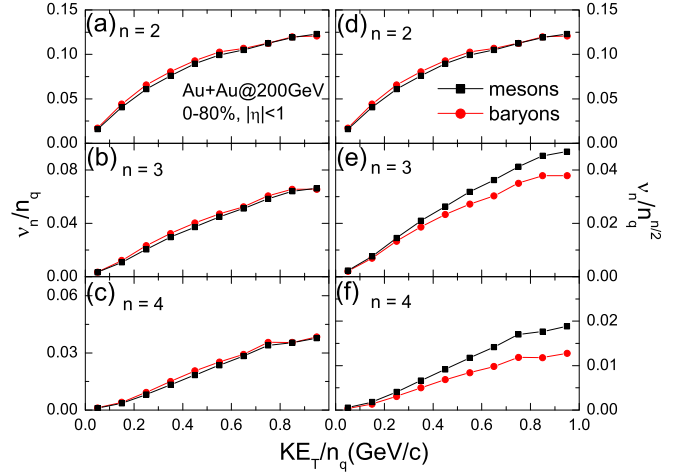


FIG. 1. Scaling relations of hadrons $v_n \sim KE_T$ in minibias Au+Au collisions at $\sqrt{s_{NN}} = 200$ GeV from the analytical coalescence scenario.

modified NCQ scaling $v_n/n_q^{n/2} \sim KE_T/n_q$. In this case events of Au+Au collisions at $\sqrt{s_{NN}} = 200$ GeV with a partonic scattering cross section of 10 mb have been generated from the AMPT model to get the information of partonic flows at freeze-out. The hadronic flow is then calculated through the analytical coalescence scenario. The mass of the hadron used in calculating the transverse kinetic energy $KE_T = \sqrt{p_T^2 + m^2} - m$ is set to be two or three times the bare quark mass in ZPC but ideally it should approach the constituent mass at hadronization, with the latter realized in a more realistic Nambu-Jona-Lasinio transport model [40,41]. According to Fig. 1, it is seen that the analytical coalescence scenario leads to the original NCQ scaling $v_n/n_q \sim KE_T/n_q$ instead of the modified one $v_n/n_q^{n/2} \sim KE_T/n_q$. This is consistent with the discussions in Sec. II B.

To understand the relation between the modified NCQ scaling $v_n/n_q^{n/2} \sim KE_T/n_q$ and the scaling relation $v_n \sim v_2^{n/2}$, we can go into further details of the results in Fig. 1 in a semianalytical way. Suppose for mesons and baryons we have the scaling relation

$$\begin{aligned} v_n &= C_n^m v_2^{n/2} \quad (\text{for mesons}), \\ v_n &= C_n^b v_2^{n/2} \quad (\text{for baryons}), \end{aligned} \quad (7)$$

for $n > 2$ with the scaling coefficients C_n^m and C_n^b for mesons and baryons, respectively. Then, if the NCQ scaling for v_2 is satisfied, i.e., $v_2/n_q = g(KE_T/n_q)$, we automatically get the modified NCQ scaling relation for higher-order flows ($n > 2$):

$$\begin{aligned} v_n^m/n_q^{n/2} &= C_n^m g^{n/2}(KE_T/n_q) \quad (\text{for mesons}), \\ v_n^b/n_q^{n/2} &= C_n^b g^{n/2}(KE_T/n_q) \quad (\text{for baryons}). \end{aligned} \quad (8)$$

The modified NCQ scaling relation is satisfied only if $C_n^m = C_n^b$, which is not the case from the analytical coalescence scenario. If the value of F_0/\tilde{F}_0 is approximated to be 1, C_n^m/C_n^b is about $\sqrt{3}/2$ for $n = 3$ and $3/2$ for $n = 4$, from the leading terms in Eqs. (A16), (A17), (A18), and (A19).

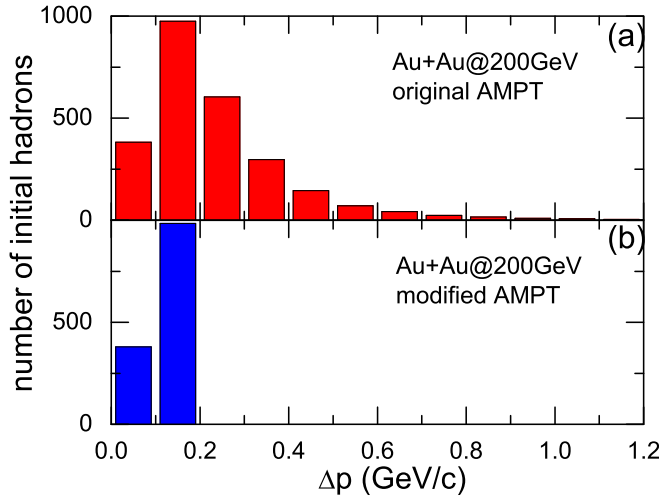


FIG. 2. Histogram of the momentum distance Δp between valence quarks in the hadronization process from the original (a) and the modified AMPT model (b) in Au+Au collisions at $\sqrt{s_{NN}} = 200$ GeV.

It has been shown that the flows of mesons and baryons from the AMPT model show a reasonable modified NCQ scaling relation in Ref. [42], although the reason has never been clarified. As we have mentioned, in the original AMPT model partons which are closer in coordinate space can coalesce into hadrons to preserve the geometry distribution, while the momentum distance Δp between valence quarks may not be small. This is displayed in the upper panel of Fig. 2, which shows that although Δp peaks around 0.2 GeV/c, it can be relatively large in some of the quark combinations. This is different from the naive analytical coalescence scenario. Using the original AMPT model, we display the scaling relation $v_n \sim KE_T$ for initial hadrons right after hadronization and final hadrons after hadronic rescatterings with a 10-mb parton scattering cross section in Fig. 3. One sees that the flows of initial hadrons do not deviate from the NCQ scaling relation

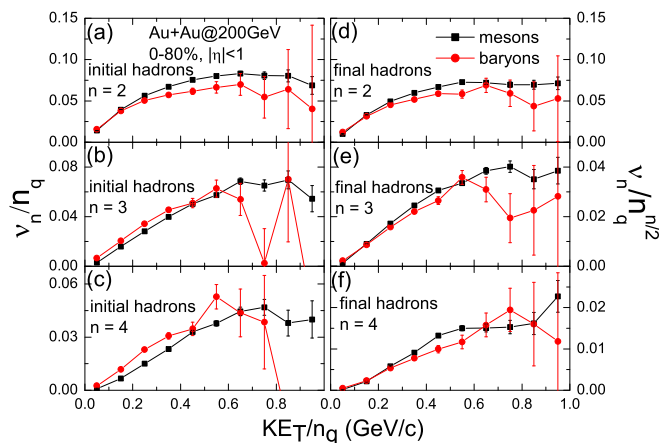


FIG. 3. Scaling relation of $v_n \sim KE_T$ for initial hadrons right after hadronization (left) and final hadrons after hadronic evolution (right) in minibias Au+Au collisions at $\sqrt{s_{NN}} = 200$ GeV from the original AMPT model.

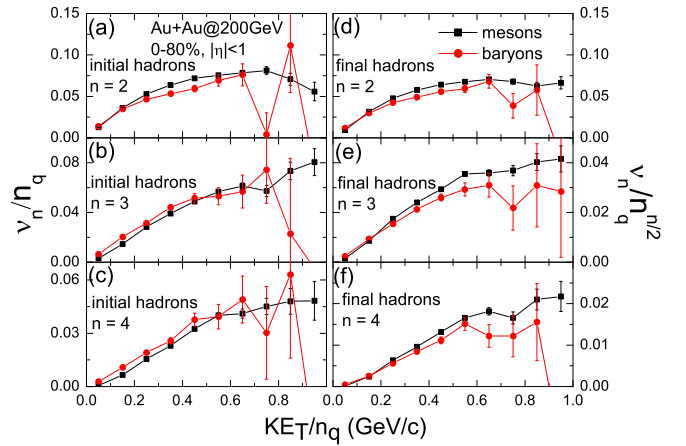


FIG. 4. Same as Fig. 3 but from the modified AMPT model.

$v_n/n_q \sim KE_T/n_q$ by much, although Δp between valence quark is not small. On the other hand, the flows of final hadrons follow reasonably well the modified NCQ scaling $v_n/n_q^{n/2} \sim KE_T/n_q$ after hadronic evolution, consistent with the results in Ref. [42].

The results from the original AMPT model did not tell us whether the modified NCQ scaling of final hadrons comes from the imperfect coalescence or the hadronic afterburner effect. To effectively study the hadronic afterburner effect with a coalescence scenario similar to the analytical one, we modified the AMPT model by abandoning the hadrons with Δp larger than 0.2 GeV/c, as displayed in the lower panel of Fig. 2. The rescatterings and decays of these hadrons in the hadronic phase are turned off, and they will not enter the flow analysis by special labeling. In this case the effective density in the hadronic phase is lower and the hadronic rescattering effect is weaker. It is seen from Fig. 4 that the flows of initial hadrons are closer to the NCQ scaling relation $v_n/n_q \sim KE_T/n_q$ compared with that from the original AMPT model shown in Fig. 3, consistent with the results from the analytical coalescence scenario except that the magnitude of the flows is slightly different, as a result of different hadron masses used in the two approaches. Despite the weaker hadronic afterburner effect compared with that from the original AMPT calculation, the flows of final hadrons again follow the relation $v_n/n_q^{n/2} \sim KE_T/n_q$, after hadronic evolution including elastic and inelastic scatterings as well as resonance decays. It is thus more believable that the hadronic afterburner can be responsible for the modified NCQ scaling.

Since the hadronic rescatterings, which further thermalize the system, can lead to the modified NCQ scaling relation, one would expect that the latter might be due to the thermalization mechanism rather than the coalescence picture. This idea can be tested with Cooper-Frye freeze-out in the hydrodynamic model or the thermal blast wave model. Similar analysis has been done in Ref. [43], and in this study we apply a generalized blast wave model including higher-order flows. The scaling relation of $v_n \sim KE_T$ is compared in Fig. 5 for pions, kaons, and protons, and the similar magnitude of v_n for different orders is due to the same flow parameter used in the generalized

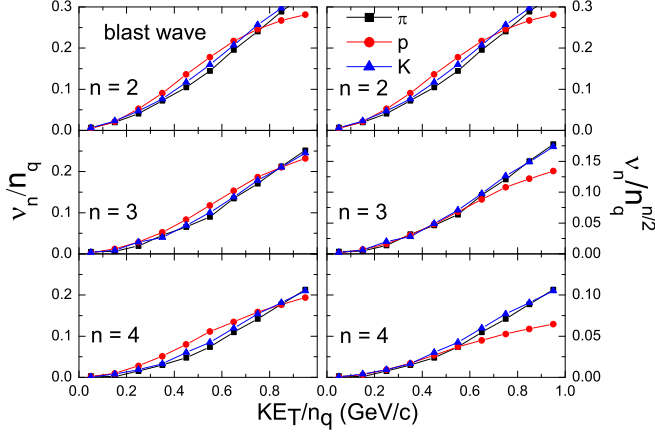


FIG. 5. Scaling relation of $v_n \sim KE_T$ for pions, kaons, and protons from a generalized blast wave model.

blast wave model as mentioned in Sec. II C. We observed the mass ordering that the flow of heavy particles is below that of lighter particles if v_n is plotted as a function of transverse momentum p_T . However, it is seen that flows of pions, kaons, and protons do not deviate from the NCQ scaling relation $v_n/n_q \sim KE_T/n_q$ by much even from a thermal blast wave model where the only difference between different particle species is their masses. On the other hand, it is observed that the modified NCQ scaling $v_n/n_q^{n/2} \sim KE_T/n_q$ is well satisfied for higher-order anisotropic flows at smaller transverse kinetic energies. It is of great interest to see whether this is the case in a more consistent hydrodynamic model and with the hadronic afterburner effect.

B. The scaling ratio $v_n/v_2^{n/2}$

The scaling relation of $v_4 \sim v_2^2$ has been observed experimentally [44–46] for many years, and it has been studied theoretically in both transport models [18,47] and hydrodynamic models [33,48,49]. The general relation of $v_n \sim v_2^{n/2}$ from consistent event plane analysis was realized only recently [29]. This scaling relation is important in understanding the initial condition [31,32] and the properties of the produced QGP [30,33]. From the analytical coalescence scenario in the present study, we will see that the scaling coefficient depends not only on the viscosity of QGP but on the hadron species as well.

With the partonic phase-space distribution at freeze-out from the AMPT model, we have obtained the anisotropic flows for hadrons via the analytical coalescence scenario and display the scaling relation of $v_n \sim v_2^{n/2}$ in Figs. 6 and 7. Figure 6 shows the centrality dependence of the $v_n/v_2^{n/2}$ ratio for $n = 3$ and 4 for partons, mesons, and baryons, and the results from partonic cross sections of 10 and 1.5 mb are compared. Compared with the ratios for partons, $v_3/v_2^{3/2}$ is about $1/\sqrt{2}$ that for mesons and about $1/\sqrt{3}$ that for baryons, and v_4/v_2^2 is about $1/2$ that for mesons and about $1/3$ that for baryons, according to Eqs. (A16), (A17), (A18), and (A19). Interestingly, from a parton scattering cross section of 10 mb, the $v_n/v_2^{n/2}$ ratio decreases with increasing centrality, as a

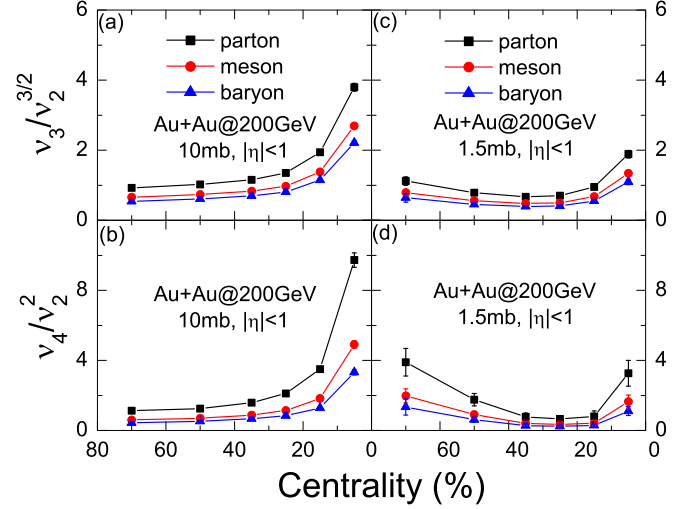


FIG. 6. Centrality dependence of $v_n/v_2^{n/2}$ for partons, mesons, and baryons in Au+Au collisions at $\sqrt{s_{NN}} = 200$ GeV from the analytical coalescence scenario with partonic flows from the parton scattering cross section of 10 mb (left) and 1.5 mb (right).

result of similar centrality dependence of the initial anisotropy ratio $\epsilon_n/\epsilon_2^{n/2}$ pointed out in Refs. [30,32]. On the other hand, from a parton scattering cross section of 1.5 mb, the correlation between the initial anisotropies ϵ_n and the final collective flows v_n is not that strong and the ratio $v_n/v_2^{n/2}$ shows a nonmonotonical dependence on the centrality. The latter case is similar to that observed from the STAR Collaboration [50] (also Figs. 4 and 5 in Ref. [49]). Figure 7 shows that the $v_n/v_2^{n/2}$ ratios for partons, mesons, and baryons are mostly independent of the transverse momentum. This is an interesting phenomena showing that the QGP interaction generates the anisotropic flows simultaneously in a p_T -independent way according to the relation $v_n/\epsilon_n \sim (v_2/\epsilon_2)^{n/2}$ from initial anisotropies

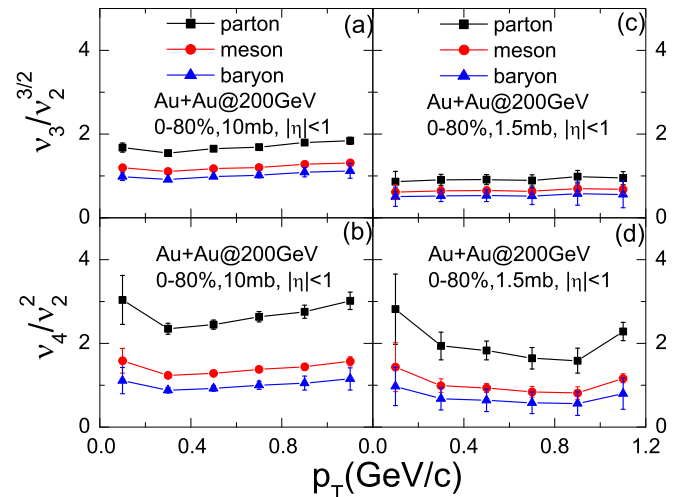


FIG. 7. Transverse momentum (p_T) dependence of $v_n(p_T)/[v_2(p_T)]^{n/2}$ in minias Au+Au collisions at $\sqrt{s_{NN}} = 200$ GeV from the analytical coalescence scenario with partonic flows from the parton scattering cross section of 10 mb (left) and 1.5 mb (right).

ϵ_n [30]. It is also interesting to see that the $v_n/v_2^{n/2}$ ratio is smaller from a parton scattering cross section of 1.5 mb compared with that of 10 mb, and the effect is larger for $n = 3$ than for $n = 4$. The insensitivity of v_4/v_2^2 to the parton scattering cross section can be due to the strong correlation between v_2 and v_4 . The $v_n/v_2^{n/2}$ ratio for partons is generated by the initial condition and the interaction of QGP, while from the analytical coalescence scenario it is guaranteed that the behavior of mesons and baryons follow the same centrality and transverse momentum dependence of that for partons. According to the previous discussion, the $v_n/v_2^{n/2}$ ratios for mesons and baryons are expected to be almost the same experimentally, since the modified NCQ scaling $v_n/n_q^{n/2} \sim K E_T/n_q$ is satisfied. To study the initial condition and the properties of QGP through the $v_n/v_2^{n/2}$ ratio, the coalescence correction is non-negligible.

In the present work, we have further investigated the effect of the hadronic afterburner on the $v_n/v_2^{n/2}$ ratio by using the original and modified AMPT model. We found that the effect of hadronic rescattering on $v_n/v_2^{n/2}$ ratio is much smaller compared with that of the partonic interaction. On the other hand, the ratios are similar for mesons and baryons after hadronic evolution from the AMPT model. This supports our previous discussion on the validity of the modified NCQ scaling law $v_n/n_q^{n/2} \sim K E_T/n_q$, which is approximately satisfied from the AMPT model calculations.

IV. CONCLUSIONS

In this work, we have investigated the modified number-of-constituent-quark (NCQ) scaling $v_n/n_q^{n/2} \sim K E_T/n_q$ and the scaling relation $v_n \sim v_2^{n/2}$. We found that the modified NCQ scaling cannot be obtained from the naive analytical coalescence scenario, which allows the coalescence of quarks only if they have the same momentum, even if event-by-event

fluctuations are taken into account. This is related to the different scaling coefficients for mesons and baryons in the scaling relation $v_n \sim v_2^{n/2}$, while experimentally they are expected to be almost the same. On the other hand, the modified NCQ scaling may stem from the hadronic afterburner effect or thermal freeze-out rather than the coalescence mechanism. The centrality dependence of the $v_n/v_2^{n/2}$ ratio has been shown to be sensitive to the parton scattering cross section, while the p_T independency of the ratio seems to be a robust phenomena. The $v_3/v_2^{3/2}$ ratio is found to be more sensitive to the partonic interaction compared with v_4/v_2^2 . Our investigation can be important in understanding the hadronization mechanism as well as the correlation between the anisotropic flows and the initial anisotropies of QGP in relativistic heavy-ion collisions.

ACKNOWLEDGMENTS

We thank C. M. Ko for helpful comments, S. Zhang for helpful discussions, and C. Zhong for maintaining the high-quality performance of the computer facility. This work was supported by the Major State Basic Research Development Program (973 Program) of China under Contracts No. 2015CB856904 and No. 2014CB845401, the National Natural Science Foundation of China under Grants No. 11475243 and No. 11421505, the 100-Talent Plan of Shanghai Institute of Applied Physics under Grants No. Y290061011 and No. Y526011011 from the Chinese Academy of Sciences, the Shanghai Key Laboratory of Particle Physics and Cosmology under Grant No. 15DZ2272100, and the Shanghai Pujiang Program under Grant No. 13PJ1410600.

APPENDIX A: HADRONIC ANISOTROPIC FLOWS FROM ANALYTICAL COALESCENCE

In this appendix, we give the expressions of the higher-order harmonic flows of hadrons based on an ideal quark coalescence scenario by considering the event-by-event initial density fluctuations. From the azimuthal distribution of partons in terms of their anisotropic flows up to the fourth order

$$f(p_T, \phi) \propto f_0 + \sum_{n=1}^4 f_n \cos[n(\phi - \psi_n)] \quad (\text{A1})$$

with $f_0 = 1$ and $f_n = 2v_n$, the azimuthal distribution of mesons in the limit that their valence quarks should have the same momentum can be expressed as

$$\begin{aligned} F(2p_T, \phi) \propto f^2(p_T, \phi) = & F_0 + 2f_0 f_1 \cos(\phi - \psi_1) + f_1 f_2 \cos(\phi + \psi_1 - 2\psi_2) + f_2 f_3 \cos(\phi + 2\psi_2 - 3\psi_3) \\ & + f_3 f_4 \cos(\phi + 3\psi_3 - 4\psi_4) + 2f_0 f_2 \cos(2\phi - 2\psi_2) + \frac{1}{2} f_1^2 \cos(2\phi - 2\psi_1) + f_1 f_3 \cos(2\phi + \psi_1 - 3\psi_3) \\ & + f_2 f_4 \cos(2\phi + 2\psi_2 - 4\psi_4) + 2f_0 f_3 \cos(3\phi - 3\psi_3) + f_1 f_2 \cos(3\phi - \psi_1 - 2\psi_2) + f_1 f_4 \cos(3\phi + \psi_1 - 4\psi_4) \\ & + 2f_0 f_4 \cos(4\phi - 4\psi_4) + \frac{1}{2} f_2^2 \cos(4\phi - 4\psi_2) + f_1 f_3 \cos(4\phi - \psi_1 - 3\psi_3) + \dots \end{aligned} \quad (\text{A2})$$

with

$$F_0 = f_0^2 + \frac{1}{2} f_1^2 + \frac{1}{2} f_2^2 + \frac{1}{2} f_3^2 + \frac{1}{2} f_4^2. \quad (\text{A3})$$

The anisotropy flows of mesons can be calculated from

$$V_n = \frac{\int_0^{2\pi} \cos(n\phi - n\psi_n) F(2p_T, \phi) d\phi}{\int_0^{2\pi} F(2p_T, \phi) d\phi}, \quad (\text{A4})$$

and their expressions for different orders are

$$V_1 = \frac{1}{F_0} \left[f_0 f_1 + \frac{1}{2} f_1 f_2 \cos(2\psi_1 - 2\psi_2) + \frac{1}{2} f_2 f_3 \cos(\psi_1 + 2\psi_2 - 3\psi_3) + \frac{1}{2} f_3 f_4 \cos(\psi_1 + 3\psi_3 - 4\psi_4) \right], \quad (\text{A5})$$

$$V_2 = \frac{1}{F_0} \left[f_0 f_2 + \frac{1}{4} f_1^2 \cos(2\psi_1 - 2\psi_2) + \frac{1}{2} f_1 f_3 \cos(\psi_1 + 2\psi_2 - 3\psi_3) + \frac{1}{2} f_2 f_4 \cos(4\psi_2 - 4\psi_4) \right], \quad (\text{A6})$$

$$V_3 = \frac{1}{F_0} \left[f_0 f_3 + \frac{1}{2} f_1 f_2 \cos(\psi_1 + 2\psi_2 - 3\psi_3) + \frac{1}{2} f_1 f_4 \cos(\psi_1 + 3\psi_3 - 4\psi_4) \right], \quad (\text{A7})$$

and

$$V_4 = \frac{1}{F_0} \left[f_0 f_4 + \frac{1}{4} f_2^2 \cos(4\psi_2 - 4\psi_4) + \frac{1}{2} f_1 f_3 \cos(\psi_1 + 3\psi_3 - 4\psi_4) \right]. \quad (\text{A8})$$

Similarly, the azimuthal distribution of baryons in the same scenario can be expressed as

$$\begin{aligned} \tilde{F}(3p_T, \phi) &\propto f^3(p_T, \phi) \\ &= \tilde{F}_0 + \left(\frac{3}{4} f_1^3 + 3 f_0^2 f_1 + \frac{3}{2} f_1 f_2^2 + \frac{3}{2} f_1 f_3^2 + \frac{3}{2} f_1 f_4^2 \right) \cos(\phi - \psi_1) + 3 f_1 f_2 \cos(\phi + \psi_1 - 2\psi_2) \\ &\quad + \frac{3}{4} f_1^2 f_3 \cos(\phi + 2\psi_1 - 3\psi_3) + \frac{3}{4} f_2^2 f_3 \cos(\phi + 3\psi_3 - 4\psi_2) + 3 f_0 f_2 f_3 \cos(\phi + 2\psi_2 - 3\psi_3) \\ &\quad + 3 f_0 f_3 f_4 \cos(\phi + 3\psi_3 - 4\psi_4) + \frac{3}{2} f_1 f_2 f_4 \cos(\phi + \psi_1 + 2\psi_2 - 4\psi_4) + \frac{3}{2} f_2 f_3 f_4 \cos(\phi - 2\psi_1 - 3\psi_3 + 4\psi_4) \\ &\quad + \left(\frac{3}{4} f_2^3 + 3 f_0^2 f_2 + \frac{3}{2} f_2 f_1^2 + \frac{3}{2} f_2 f_3^2 + \frac{3}{2} f_2 f_4^2 \right) \cos(2\phi - 2\psi_2) + \frac{3}{2} f_0 f_1^2 \cos(2\phi - 2\psi_1) \\ &\quad + \frac{3}{4} f_2^2 f_4 \cos(2\phi + 2\psi_1 - 4\psi_4) + \frac{3}{4} f_3^2 f_4 \cos(2\phi - 6\psi_3 + 4\psi_4) + 3 f_0 f_1 f_3 \cos(2\phi + \psi_1 - 3\psi_3) \\ &\quad + 3 f_0 f_2 f_4 \cos(2\phi + 2\psi_2 - 4\psi_4) + \frac{3}{2} f_1 f_2 f_3 \cos(2\phi - \psi_1 + 2\psi_2 - 3\psi_3) + \frac{3}{2} f_1 f_3 f_4 \cos(2\phi - \psi_1 + 3\psi_3 - 4\psi_4) \\ &\quad + \left(\frac{3}{4} f_3^3 + 3 f_0^2 f_3 + \frac{3}{2} f_3 f_1^2 + \frac{3}{2} f_3 f_2^2 + \frac{3}{2} f_3 f_4^2 \right) \cos(3\phi - 3\psi_3) + \frac{1}{4} f_1^3 \cos(3\phi - 3\psi_1) \\ &\quad + \frac{3}{4} f_1 f_2^2 \cos(3\phi + \psi_1 - 4\psi_2) + 3 f_1 f_2 \cos(3\phi - \psi_1 - 2\psi_2) + 3 f_0 f_1 f_4 \cos(3\phi + \psi_1 - 4\psi_4) \\ &\quad + \frac{3}{2} f_1 f_2 f_4 \cos(3\phi - \psi_1 + 2\psi_2 - 4\psi_4) + \frac{3}{2} f_2 f_3 f_4 \cos(3\phi - \psi_2 + 3\psi_3 - 4\psi_4) \\ &\quad + \left(\frac{3}{4} f_4^3 + 3 f_0^2 f_4 + \frac{3}{2} f_4 f_1^2 + \frac{3}{2} f_4 f_2^2 + \frac{3}{2} f_4 f_3^2 \right) \cos(4\phi - 4\psi_4) + \frac{3}{2} f_0 f_2^2 \cos(4\phi - 4\psi_2) \\ &\quad + \frac{3}{4} f_1^2 f_1 \cos(4\phi - 2\psi_1 - 2\psi_2) + 3 f_0 f_1 f_3 \cos(4\phi - \psi_1 - 3\psi_3) \\ &\quad + \frac{3}{2} f_1 f_2 f_3 \cos(4\phi + \psi_1 - 2\psi_2 - 3\psi_3) + \frac{3}{4} f_3^2 f_2 \cos(4\phi + 2\psi_2 - 6\psi_3) + \dots \end{aligned} \quad (\text{A9})$$

with

$$\begin{aligned} \tilde{F}_0 &= f_0^3 + \frac{3}{2} f_0 f_1^2 + \frac{3}{2} f_0 f_2^2 + \frac{3}{2} f_0 f_3^2 + \frac{3}{2} f_0 f_4^2 + \frac{3}{4} f_1^2 f_2 \cos(2\psi_1 - 2\psi_2) + \frac{3}{2} f_1 f_2 f_3 \cos(\psi_1 + 2\psi_2 - 3\psi_3) \\ &\quad + \frac{3}{4} f_2^2 f_4 \cos(4\psi_2 - 4\psi_4) + \frac{3}{2} f_1 f_3 f_4 \cos(\psi_1 + 3\psi_3 - 4\psi_4). \end{aligned} \quad (\text{A10})$$

The anisotropic flows of baryons can be calculated from

$$\tilde{V}_n = \frac{\int_0^{2\pi} \cos(n\phi - n\psi_n) \tilde{F}(3p_T, \phi) d\phi}{\int_0^{2\pi} \tilde{F}(3p_T, \phi) d\phi}, \quad (\text{A11})$$

and their detailed expressions are

$$\begin{aligned} \tilde{V}_1 &= \frac{1}{\tilde{F}_0} \left[\frac{3}{2} f_1 f_0^2 + \frac{3}{8} f_1^3 + \frac{3}{4} f_1 f_2^2 + \frac{3}{4} f_1 f_3^2 + \frac{3}{4} f_1 f_4^2 + \frac{3}{2} f_1 f_2 \cos(2\psi_1 - 2\psi_2) + \frac{3}{8} f_1^2 f_3 \cos(3\psi_1 - 3\psi_3) \right. \\ &\quad + \frac{3}{8} f_1^2 f_3 \cos(3\psi_1 - 3\psi_3) + \frac{3}{8} f_2^2 f_3 \cos(\psi_1 + 3\psi_3 - 4\psi_2) + \frac{3}{2} f_0 f_2 f_3 \cos(\psi_1 + 2\psi_2 - 3\psi_3) \\ &\quad \left. + \frac{3}{4} f_1 f_2 f_4 \cos(2\psi_1 + 2\psi_2 - 4\psi_4) + \frac{3}{2} f_0 f_3 f_4 \cos(\psi_1 + 3\psi_3 - 4\psi_4) + \frac{3}{4} f_2 f_3 f_4 \cos(\psi_1 - 2\psi_2 - 3\psi_3 + 4\psi_4) \right], \end{aligned} \quad (\text{A12})$$

$$\begin{aligned}\tilde{V}_2 = & \frac{1}{\tilde{F}_0} \left[\frac{3}{2} f_2 f_0^2 + \frac{3}{8} f_2^3 + \frac{3}{4} f_2 f_1^2 + \frac{3}{4} f_2 f_3^2 + \frac{3}{4} f_2 f_4^2 + \frac{3}{4} f_0 f_1^2 \cos(2\psi_1 - 2\psi_2) + \frac{3}{8} f_1^2 f_4 \cos(2\psi_1 + 2\psi_2 - 4\psi_4) \right. \\ & + \frac{3}{4} f_3^2 f_4 \cos(2\psi_2 + 4\psi_4 - 6\psi_3) + \frac{3}{2} f_0 f_1 f_3 \cos(\psi_1 + 2\psi_2 - 3\psi_3) + \frac{3}{4} f_1 f_2 f_3 \cos(\psi_1 + 3\psi_3 - 4\psi_2) \\ & \left. + \frac{3}{2} f_0 f_2 f_4 \cos(4\psi_2 - 4\psi_4) + \frac{3}{4} f_1 f_3 f_4 \cos(\psi_1 - 2\psi_2 - 3\psi_3 + 4\psi_4) \right],\end{aligned}\quad (\text{A13})$$

$$\begin{aligned}\tilde{V}_3 = & \frac{1}{\tilde{F}_0} \left[\frac{3}{2} f_3 f_0^2 + \frac{3}{8} f_3^3 + \frac{3}{4} f_3 f_1^2 + \frac{3}{4} f_3 f_2^2 + \frac{3}{4} f_3 f_4^2 + \frac{3}{8} f_1^3 \cos(3\psi_1 - 3\psi_3) + \frac{3}{8} f_2^2 f_1 \cos(\psi_1 + 3\psi_3 - 4\psi_2) \right. \\ & + \frac{3}{2} f_1 f_2 \cos(\psi_1 + 2\psi_2 - 3\psi_3) + \frac{3}{2} f_0 f_1 f_4 \cos(\psi_1 + 3\psi_3 - 4\psi_4) + \frac{3}{4} f_2 f_3 f_4 \cos(2\psi_2 + 4\psi_4 - 6\psi_3) \\ & \left. + \frac{3}{4} f_1 f_2 f_4 \cos(\psi - 2\psi_2 - 3\psi_3 + 4\psi_4) \right],\end{aligned}\quad (\text{A14})$$

and

$$\begin{aligned}\tilde{V}_4 = & \frac{1}{\tilde{F}_0} \left[\frac{3}{2} f_4 f_0^2 + \frac{3}{8} f_4^3 + \frac{3}{4} f_4 f_1^2 + \frac{3}{4} f_4 f_2^2 + \frac{3}{4} f_4 f_3^2 + \frac{3}{4} f_0 f_2^2 \cos(4\psi_2 - 4\psi_4) + \frac{3}{8} f_1^2 f_2 \cos(2\psi_1 + 2\psi_2 - 4\psi_4) \right. \\ & \left. + \frac{3}{2} f_0 f_1 f_3 \cos(\psi_1 + 3\psi_3 - 4\psi_4) + \frac{3}{4} f_1 f_2 f_3 \cos(\psi_1 - 2\psi_2 - 3\psi_3 + 4\psi_4) + \frac{3}{8} f_2 f_3^2 \cos(2\psi_2 + 4\psi_4 - 6\psi_3) \right].\end{aligned}\quad (\text{A15})$$

Here we only consider the flows up to the fourth order; thus the even higher-order terms in Eqs. (A2) and (A9) do not contribute.

To investigate the scaling relation between flows of different orders $v_n \sim v_2^{n/2}$, we also give the expressions of the corresponding ratios in the analytical coalescence scenario. The ratios of $V_n/V_2^{n/2}$ for mesons with $n = 3$ and 4 by neglecting the higher-order terms can be written as

$$\frac{V_3}{V_2^{3/2}} \approx F_0^{1/2} \left[\frac{1}{\sqrt{2}} \frac{v_3}{v_2^{3/2}} + \frac{1}{\sqrt{2}} \frac{v_1}{v_2^{1/2}} \cos(\psi_1 + 2\psi_2 - 3\psi_3) + \frac{1}{\sqrt{2}} \frac{v_1 v_4}{v_2^{3/2}} \cos(\psi_1 + 3\psi_3 - 4\psi_4) \right],\quad (\text{A16})$$

$$\frac{V_4}{V_2^2} \approx F_0 \left[\frac{1}{2} \frac{v_4}{v_2^2} + \frac{1}{4} \cos(4\psi_2 - 4\psi_4) + \frac{1}{2} \frac{v_1 v_3}{v_2^2} \cos(\psi_1 + 3\psi_3 - 4\psi_4) \right].\quad (\text{A17})$$

The ratios of $\tilde{V}_n/\tilde{V}_2^{n/2}$ for baryons with $n = 3$ and 4 by neglecting the higher-order terms can be written as

$$\begin{aligned}\frac{\tilde{V}_3}{\tilde{V}_2^{3/2}} \approx & \tilde{F}_0^{1/2} \left[\frac{1}{\sqrt{3}} \frac{v_3}{v_2^{3/2}} + \frac{1}{\sqrt{3}} \frac{v_3^3}{v_2^{3/2}} + \frac{2}{\sqrt{3}} \frac{v_3 v_1^2}{v_2^{3/2}} + \frac{2}{\sqrt{3}} v_3 v_2^{1/2} + \frac{2}{\sqrt{3}} \frac{v_3 v_4^2}{v_2^{3/2}} + \frac{1}{\sqrt{3}} \frac{v_1^3}{v_2^{3/2}} \cos(3\psi_1 - 3\psi_3) \right. \\ & + \frac{1}{\sqrt{3}} v_2^{1/2} v_1 \cos(\psi_1 + 3\psi_3 - 4\psi_2) + \frac{2}{\sqrt{3}} \frac{v_1}{v_2^{1/2}} \cos(\psi_1 + 2\psi_2 - 3\psi_3) + \frac{2}{\sqrt{3}} \frac{v_1 v_4}{v_2^{3/2}} \cos(\psi_1 + 3\psi_3 - 4\psi_4) \\ & \left. + \frac{2}{\sqrt{3}} \frac{v_3 v_4}{v_2^{1/2}} \cos(2\psi_2 + 4\psi_4 - 6\psi_3) + \frac{2}{\sqrt{3}} \frac{v_1 v_4}{v_2^{1/2}} \cos(\psi_1 - 2\psi_2 - 3\psi_3 + 4\psi_4) \right],\end{aligned}\quad (\text{A18})$$

$$\begin{aligned}\frac{\tilde{V}_4}{\tilde{V}_2^2} \approx & \tilde{F}_0 \left[\frac{1}{3} \frac{v_4}{v_2^2} + \frac{1}{3} \frac{v_4^3}{v_2^2} + \frac{2}{3} \frac{v_4 v_1^2}{v_2^2} + \frac{2}{3} v_4 + \frac{2}{3} \frac{v_4 v_3^2}{v_2^2} + \frac{1}{3} \cos(4\psi_2 - 4\psi_4) + \frac{1}{3} \frac{v_1^2}{v_2} \cos(2\psi_1 + 2\psi_2 - 4\psi_4) \right. \\ & \left. + \frac{2}{3} \frac{v_1 v_3}{v_2^2} \cos(\psi_1 + 3\psi_3 - 4\psi_4) + \frac{1}{3} \frac{v_2^2}{v_2} \cos(2\psi_2 + 4\psi_4 - 6\psi_3) + \frac{2}{3} \frac{v_1 v_3}{v_2} \cos(\psi_1 - 2\psi_2 - 3\psi_3 + 4\psi_4) \right].\end{aligned}\quad (\text{A19})$$

APPENDIX B: ANISOTROPIC FLOWS FROM EVENT PLANE METHOD

Here we briefly review the standard method of calculating the anisotropic flows as well as the event plane from particle freeze-out distribution in the present work. We refer the readers to Refs. [51,52] for more details.

We start from the momentum distribution of emitted particles as follows:

$$E \frac{d^3 N}{d^3 p} = \frac{1}{2\pi} \frac{d^2 N}{p_T d p_T dy} \left\{ 1 + \sum_{n=1}^{\infty} 2v_n \cos[n(\phi - \psi_n)] \right\},\quad (\text{B1})$$

where ϕ is the azimuthal angle of emitted particles, y and p_T are respectively the rapidity and transverse momentum, v_n is the n th-order anisotropic flows, and ψ_n is the corresponding event plane angle. The relation between the event flow vector Q_n and the event plane angle ψ_n can be expressed as

$$Q_{n,x} = Q_n \cos(n\psi_n) = \sum_i \omega_i \cos(n\phi_i), \quad (\text{B2})$$

$$Q_{n,y} = Q_n \sin(n\psi_n) = \sum_i \omega_i \sin(n\phi_i), \quad (\text{B3})$$

where the summation goes over all particles i used in the event plane calculation, and ϕ_i and ω_i are respectively the azimuthal angle and the weight factor for particle i , with the latter set as the transverse momentum of the particle. The event plane angle can thus be calculated from

$$\psi_n = \left[\text{atan2} \frac{\sum_i \omega_i \sin(n\phi_i)}{\sum_i \omega_i \cos(n\phi_i)} \right] / n. \quad (\text{B4})$$

The n th-order flow magnitude v_n^{obs} with respect to this event plane is

$$v_n^{obs}(p_T, y) = \langle \cos[n(\phi_i - \psi_n)] \rangle, \quad (\text{B5})$$

where $\langle \dots \rangle$ denotes an average over all particles in all events with their azimuthal angle ϕ_i for a given rapidity y and transverse momentum p_T . To remove autocorrelations, one has to subtract the contribution of the particle of interest from the total Q_n vector, obtaining a ψ_n uncorrelated with that particle. Since finite multiplicity limits the estimation of the

event plane angle, v_n has to be corrected by the event plane resolution for each n given by

$$\mathfrak{R}_n(\chi) = \frac{\sqrt{\pi}}{2} \chi \exp(-\chi^2/2) [I_{(k-1)/2}(\chi^2/2) + I_{(k+1)/2}(\chi^2/2)], \quad (\text{B6})$$

where we have $\chi = v_n \sqrt{M}$ with M being the particle multiplicity, and I_k is the modified Bessel function. To calculate the event plane resolution, the full events are divided up into two independent subevents of equal multiplicity. Thus the resolution for subevents is just the square root of this correlation defined as

$$\mathfrak{R}_n^{sub} = \sqrt{\langle \cos[n(\psi_n^A - \psi_n^B)] \rangle}, \quad (\text{B7})$$

where A and B denote the two subgroups of particles. In our calculation we divided particles within pseudorapidity window $|\eta| < 1$ into two groups of forward and backward spheres with a gap of $|\Delta\eta| < 0.1$. The full event plane resolution is obtained by

$$\mathfrak{R}_n^{full} = \mathfrak{R}(\sqrt{2}\chi_{sub}), \quad (\text{B8})$$

where χ_{sub} is inversely obtained from the subevent resolution \mathfrak{R}_n^{sub} via Eq. (B6). The final anisotropic flow is

$$v_n = \frac{v_n^{obs}(p_T, y)}{\mathfrak{R}_n^{full}}. \quad (\text{B9})$$

-
- [1] I. Arsene *et al.* (PHOBOS Collaboration), *Nucl. Phys. A* **757**, 1 (2005).
- [2] B. B. Back *et al.* (BRAHMS Collaboration), *Nucl. Phys. A* **757**, 28 (2005).
- [3] J. Adams *et al.* (STAR Collaboration), *Nucl. Phys. A* **757**, 102 (2005).
- [4] K. Adcox *et al.* (PHENIX Collaboration), *Nucl. Phys. A* **757**, 184 (2005).
- [5] J. Adams *et al.* (STAR Collaboration), *Phys. Rev. Lett.* **92**, 052302 (2004).
- [6] J. Adams *et al.* (STAR Collaboration), *Phys. Rev. C* **72**, 014904 (2005).
- [7] J. Adams *et al.* (STAR Collaboration), *Phys. Rev. Lett.* **95**, 122301 (2005).
- [8] A. Adare *et al.* (PHENIX Collaboration), *Phys. Rev. Lett.* **98**, 162301 (2007).
- [9] A. Adare *et al.* (PHENIX Collaboration), *Phys. Rev. Lett.* **99**, 052301 (2007).
- [10] J. Adams *et al.* (STAR Collaboration), *Phys. Rev. C* **77**, 054901 (2008).
- [11] V. Greco, C. M. Ko, and P. Lévai, *Phys. Rev. Lett.* **90**, 202302 (2003).
- [12] V. Greco, C. M. Ko, and P. Lévai, *Phys. Rev. C* **68**, 034904 (2003).
- [13] R. J. Fries, B. Müller, C. Nonaka, and S. A. Bass, *Phys. Rev. Lett.* **90**, 202303 (2003).
- [14] R. J. Fries, B. Müller, C. Nonaka, and S. A. Bass, *Phys. Rev. C* **68**, 044902 (2003).
- [15] R. C. Hwa and C. B. Yang, *Phys. Rev. C* **67**, 064902 (2003).
- [16] D. Molnár and S. A. Voloshin, *Phys. Rev. Lett.* **91**, 092301 (2003).
- [17] P. F. Kolb, L. W. Chen, V. Greco, and C. M. Ko, *Phys. Rev. C* **69**, 051901(R) (2004).
- [18] L. W. Chen, C. M. Ko, and Z. W. Lin, *Phys. Rev. C* **69**, 031901(R) (2004).
- [19] F. Retière and M. A. Lisa, *Phys. Rev. C* **70**, 044907 (2004).
- [20] F. Cooper and G. Frye, *Phys. Rev. D* **10**, 186 (1974).
- [21] B. Alver and G. Roland, *Phys. Rev. C* **81**, 054905 (2010).
- [22] B. H. Alver, C. Gombeaud, M. Luzum, and J. Y. Ollitrault, *Phys. Rev. C* **82**, 034913 (2010).
- [23] H. Petersen, G. Y. Qin, S. A. Bass, and B. Müller, *Phys. Rev. C* **82**, 041901 (2010).
- [24] B. Schenke, S. Jeon, and C. Gale, *Phys. Rev. Lett.* **106**, 042301 (2011).
- [25] J. Xu and C. M. Ko, *Phys. Rev. C* **83**, 021903(R) (2011).
- [26] J. Xu and C. M. Ko, *Phys. Rev. C* **84**, 014903 (2011).
- [27] G. L. Ma and X. N. Wang, *Phys. Rev. Lett.* **106**, 162301 (2011).
- [28] A. Adare *et al.* (PHENIX Collaboration), arXiv:1412.1038v1 [nucl-ex].
- [29] G. Aad *et al.* (ATLAS Collaboration), *Phys. Rev. C* **86**, 014907 (2012).
- [30] R. A. Lacey, A. Taranenko, J. Jia, N. N. Ajitanand, and J. M. Alexander, arXiv:1105.3782v2 [nucl-ex].
- [31] R. A. Lacey, R. Wei, N. N. Ajitanand, J. M. Alexander, X. Gong, J. Jia, A. Taranenko, R. Pak, and H. Stöcker, *Phys. Rev. C* **81**, 061901 (2010).

- [32] R. A. Lacey, R. Wei, J. Jia, N. N. Ajitanand, J. M. Alexander, and A. Taranenko, *Phys. Rev. C* **83**, 044902 (2011).
- [33] F. G. Gardim, F. Grassi, M. Luzum, and J.-Y. Ollitrault, *Phys. Rev. Lett.* **109**, 202302 (2012).
- [34] Z. W. Lin, C. M. Ko, B. A. Li, B. Zhang, and S. Pal, *Phys. Rev. C* **72**, 064901 (2005).
- [35] X. N. Wang and M. Gyulassy, *Phys. Rev. D* **44**, 3501 (1991).
- [36] B. Zhang, *Comput. Phys. Commun.* **109**, 193 (1998).
- [37] B. A. Li and C. M. Ko, *Phys. Rev. C* **52**, 2037 (1995).
- [38] L. W. Chen, C. M. Ko, and B. A. Li, *Phys. Rev. C* **68**, 017601 (2003); *Nucl. Phys. A* **729**, 809 (2003).
- [39] Y. Oh, Z. W. Lin, and C. M. Ko, *Phys. Rev. C* **80**, 064902 (2009).
- [40] T. Song, S. Plumari, V. Greco, C. M. Ko, and F. Li, [arXiv:1211.5511](https://arxiv.org/abs/1211.5511) [nucl-th].
- [41] J. Xu, T. Song, C. M. Ko, and F. Li, *Phys. Rev. Lett.* **112**, 012301 (2014).
- [42] L. X. Han, G. L. Ma, Y. G. Ma, X. Z. Cai, J. H. Chen, S. Zhang, and C. Zhong, *Phys. Rev. C* **84**, 064907 (2011).
- [43] S. Pratt and S. Pal, *Phys. Rev. C* **71**, 014905 (2005).
- [44] J. Adams *et al.* (STAR Collaboration), *Phys. Rev. Lett.* **92**, 062301 (2004).
- [45] B. I. Abelev *et al.* (STAR Collaboration), *Phys. Rev. C* **75**, 054906 (2007).
- [46] A. Adare *et al.* (PHENIX Collaboration), *Phys. Rev. Lett.* **105**, 062301 (2010).
- [47] V. P. Konchakovski, E. L. Bratkovskaya, W. Cassing, V. D. Toneev, S. A. Voloshin, and V. Voronyuk, *Phys. Rev. C* **85**, 044922 (2012).
- [48] N. Borghini and J.-Y. Ollitrault, *Phys. Lett. B* **642**, 227 (2006).
- [49] C. Gombeaud and J.-Y. Ollitrault, *Phys. Rev. C* **81**, 014901 (2010).
- [50] Y. Bai, PhD thesis, NIKHEF and Utrecht University, 2007 (unpublished).
- [51] A. M. Poskanzer and S. A. Voloshin, *Phys. Rev. C* **58**, 1671 (1998).
- [52] S. A. Voloshin, A. M. Poskanzer, and R. Snellings, [arXiv:0809.2949](https://arxiv.org/abs/0809.2949) [nucl-ex].